Chapter One: An Introduction to Nonlinear Optics, Second Order Nonlinear Applications, and Nonlinear Materials

This thesis presents an investigation into a novel organic polymer nanoscale film deposition technique, detailing its potential for producing second-order nonlinear optical materials. The goal of this study is to establish how deposition parameters affect film formation in the Ionic Self-Assembled Monolayer (ISAM) technique, to characterize the properties of this technique which make ISAM deposition particularly useful for fabrication of second-order nonlinear materials, and to suggest possible improvements that will make ISAM films capable of incorporation into optoelectronic device applications.

Since the initial observation in 1961 of second harmonic generation from a quartz crystal pumped by a ruby laser[1], second order non-linear optical effects have been of great interest. Frequency mixing capabilities are routinely used in laboratory settings to convert laser wavelengths to different regions of interest. An effect that is perhaps even more important from an applications perspective is the electro-optic effect. Its implementations have been limited, however, by the high cost associated with current state-of-the-art materials. The electro-optic effect utilizes a DC electric field to change the refractive index in the medium. This capability allows the construction of many types of light modulators and switches. While in the computing and communications industry today much of the data transmission is conducted by fiber optics, most of the switching is done electronically. Electronic signals are fed into laser diodes which send the information down a fiber optic cable, where it is eventually received by a photodetector and processed electronically. The use of fiber optics greatly expands signal bandwidth, but processing times are still slow, and conversion processes consume great amounts of energy and dissipate large amounts of heat. Electro-optic devices allow the possibility of easily switching and modulating light signals, eliminating much of the current need for electronic processing.

While such modulators have been built and are marketed, the materials generally used (inorganic crystals) are very expensive due to complicated and time-consuming fabrication processes. As a possible

alternative, organic chromophore 'dyes' possess strong second-order nonlinear capabilities, and can be incorporated as thin-films into devices for application. To be of use as a second-order material, however, a method for producing a net non-centrosymmetry in the medium must be employed. This has most commonly been achieved through guest-host polymer films, in which the chromophores do not possess an inherent order, but rather are aligned by the application of an external electric field and 'frozen' into place. While this effect has produced strong nonlinear susceptibilities, comparable to and in some cases exceeding those of the inorganic crystals, this induced alignment is thermally fragile, decaying over time and with increased temperature.

As a possible replacement, this study presents a novel technique[2] for producing films in which the chromophores self-align into inherently non-centrosymmetric structures. The ionic self-assembled monolayer (ISAM) technique utilizes coulombic interactions between polyelectrolytes to produce thin polymer films that can have significant second-order nonlinear susceptibilities.

Absorbance and film thickness measurements have allowed a general physical description of film formation and how film structure is affected by solution parameters such as pH and ionic strength. We have observed that film thickness is a function of the electrostatic screening of the polymer in solution. This screening can be the result of increased ionic strength, where the presence of small ions in solution 'dilutes' the local electrostatic neighborhood, or a function of pH when polymers are marginally soluble, for similar reasons. Studies of the solution immersion time required for film formation have given us some insight into the kinematics of polyelectrolyte adsorption. We have found that film formation occurs quickly, reaching an equilibrium thickness within 45 seconds of immersion. After this time, very little additional polymer is adsorbed.

The primary focus of this study is the measurement of the second order nonlinear optical susceptibility. These are made by measurements of second harmonic generation in the films. Second harmonic generation is then used as a probe of the film structure to determine the chromophore structure and orientation. From these measurements we find that only some of the chromophores present in the film contribute to the

nonlinearity of the medium. These chromophores are located at the interfaces between successive layers. The vast majority of chromophores present are randomly aligned and do not contribute to the second order susceptibility. Most importantly for application purposes, we find that ISAM films exhibit great thermal stability at elevated temperatures and most remarkably, complete recovery of the second order nonlinearity as the films cool back down to room temperature. At room temperature, the second order nonlinear susceptibility is stable over a period of time greater than two years.

Lastly we make an initial study of some methods to increase the nonlinearity associated with ISAM films. The use of specially tailored chromophores with large hyperpolarizabilities is one approach to achieve this end. A possibility for decreasing the average chromophore tilt angle (thus increasing nonlinearity) lies in complexing the polymer chromophores with cyclodextrins, forming pseudorotaxanes. Our first implementation of this technique was not very successful due (most likely) to a poor choice of polymer chromophore. We also show initial results from a structural variation of ISAM deposition. This process uses dianionic chromophore molecules in place of a polyanion in the deposition procedure. This should decrease the 'loss' of nonlinear susceptibility due to randomly oriented chromophores and the competition of oppositely oriented chromophores. Our initial studies indicate that the expected adsorption of material is taking place in a linear fashion, but second harmonic generation results are not as good as expected. Suggestions will be made for methods of making these novel approaches more successful.

1.1 A Brief Introduction to Nonlinear Optics

Optics is the study of the interaction of electromagnetic radiation and matter. Electromagnetic radiation is described by Maxwell's equations

$$\nabla \cdot \vec{D} = 4\pi\rho$$
$$\nabla \times \vec{H} - \frac{1}{c}\frac{\partial \vec{D}}{\partial t} = \frac{4\pi}{c}\vec{J} \qquad (1.1.1)$$
$$\nabla \times \vec{E} + \frac{1}{c}\frac{\partial \vec{B}}{\partial t} = 0$$
$$\nabla \cdot \vec{B} = 0$$

The electric displacement field $\vec{D}$ is related to the electric field $\vec{E}$ through the polarization field $\vec{P}$ in a medium

$$\vec{D} = \vec{E} + 4\pi\vec{P} \qquad (1.1.2)$$

Most often, the polarization field is considered to be linearly related to the incident electric field

$$\vec{P} = \chi\vec{E} \qquad (1.1.3)$$

Where the electrical susceptibility, χ, is a second-rank tensor. While this consideration tends to be sufficient when relating incident fields at low field strengths, it is a simplification and not completely correct. In reality, the polarization field is more complicated than the linear relation given above. If the variation is small, the polarization may be expanded in a Taylor series to obtain

$$\vec{P} = \chi^{(1)}\vec{E} + \chi^{(2)}\vec{E}^2 + \chi^{(3)}\vec{E}^3 + \cdots \qquad (1.1.4a)$$

$$P_i = \chi_{ij}^{(1)}E_j + \chi_{ijk}^{(2)}E_jE_k + \chi_{ijkl}^{(3)}E_jE_kE_l + \cdots \qquad (1.1.4b)$$

where terms are summed over repeated indices. The first coefficient, $\chi_{ij}^{(1)}$ is the linear electric susceptibility discussed previously. The other $\chi^{(n)}$ are called the n^{th} order nonlinear susceptibilities.

As an example, consider the interaction of an optical electric field at frequency ω and amplitude E_ω

$$E_\omega(t) = E_\omega(e^{+i\omega t} + e^{-i\omega t}) \qquad (1.1.5)$$

with a static electric field E_o in a medium with a nonzero $\chi^{(2)}$. The second-order polarization field in this medium is (from eq. 1.1.4a)

$$\begin{aligned}\vec{P}^{(2)}(t) &= \chi^{(2)}\vec{E}^{2}(t) \\ &= \chi^{(2)}\left[E_\omega e^{+i\omega t} + E_\omega e^{-i\omega t} + E_o\right]^2 \\ &= \chi^{(2)}\left[E_\omega^2\left(e^{+i2\omega t} + e^{-i2\omega t}\right)\right. \\ &\quad + 2E_o E_\omega\left(e^{+i\omega t} + e^{-i\omega t}\right) \\ &\quad \left. + 2E_\omega^2 + E_o^2\right]\end{aligned} \tag{1.1.6}$$

The resulting polarization field contains components oscillating at various frequencies. The first term in eq. (1.1.6) oscillates at 2ω and may radiate light at that frequency. This term depends only on the presence of the field at frequency ω and not on the static field. This effect is referred to as second harmonic generation (SHG). The second term in eq. 1.1.6 oscillates at ω and causes a variation in the refractive index in the medium. This effect, the linear electro-optic effect, will be discussed shortly. The third term does not oscillate in time. This is known as optical rectification, and is a conversion of an oscillating electric field to a static DC field.

These and other phenomena arise from a mixing of applied frequencies in a non-linear medium. Because the nature of the polarization field is dependent on the incident electric fields, the effects resulting from the nonlinear susceptibilities are given a shorthand notation denoted by the appropriate order susceptibility and incident and resultant electric field frequencies. Eq. 1.1.4b is rewritten (for the second order susceptibility) as

$$P_i^{(2)} = \chi_{ijk}^{(2)}\left(-\omega_3;\omega_1,\omega_2\right)E_j^{\omega_1}E_k^{\omega_2} \tag{1.1.7}$$

where indices i,j,k denote cartesian components of electric fields oscillating at $\omega_3,\omega_2,\omega_1$, respectively. The frequencies are related such that

$$\omega_3 = (\omega_1 + \omega_2) \tag{1.1.8}$$

where ω_3 is the 'output' frequency and ω_1 and ω_2 are the frequencies of the incident electric fields. Some of the effects characterized by the second order susceptibility are:

$\chi_{ijk}^{(2)}(-2\omega;\omega;\omega)$ Second Harmonic Generation (SHG)

$\chi_{ijk}^{(2)}(-\omega;\omega;0)$ Linear Electro-optic Effect (LEO)

$\chi^{(2)}_{ijk}(-\omega_1 - \omega_2; \omega_1; \omega_2)$ Sum Frequency Generation (SFG)

$\chi^{(2)}_{ijk}(-\omega_1 + \omega_2; \omega_1; \omega_2)$ Difference Frequency Generation (DFG)

The nonlinear polarizations act as source terms in the optical wave equation[3]

$$\nabla^2 E - \frac{n^2}{c^2}\frac{\partial^2 E}{\partial t^2} = \frac{4\pi}{c^2}\frac{\partial^2 P}{\partial t^2} \tag{1.1.9}$$

so the polarization fields arising from these susceptibilities generate electromagnetic radiation that is observable and can be utilized in practical application.

1.2 Applications of Second Order Non-Linear Optical Materials

One of the most widely used applications for nonlinear media is the generation of second harmonic radiation. As illustrated above (eq. 1.1.6), radiation at frequency ω is converted into radiation at frequency 2ω within the nonlinear medium. This process generally occurs through virtual transitions where two photons at ω are simultaneously destroyed while a single photon at 2ω is created in a single quantum mechanical process. This process can result in nearly complete conversion of the incident fundamental energy into the second harmonic, and is used extensively in the laboratory to obtain coherent optical radiation with wavelengths other than the fundamental of the fixed-wavelength laser source. Phase-matching concerns as well as the use of second harmonic generation as a probe technique will be discussed in Chapter 3.

For the case of a linear medium with $\vec{P} = \chi^{(1)}\vec{E}$, eq. (1.1.2) and (1.1.3) give a displacement field

$$\vec{D} = \vec{E} + 4\pi\chi^{(1)}\vec{P} = (1 + 4\pi\chi^{(1)})\vec{E} \tag{1.2.1}$$

Since

$$\vec{D} = \varepsilon\vec{E} \tag{1.2.2}$$

and $n_o = \sqrt{\varepsilon}$, we can write the refractive index n_1 for a linear medium

$$n_o = \sqrt{1 + 4\pi\chi^{(1)}} \tag{1.2.3}$$

The refractive index in this case is clearly independent of the applied field, though since $\chi^{(1)}$ is a second-rank tensor, the index can depend on the polarization of the wave.

Recall the second order polarization field for a non-centrosymmetric medium from eq. 1.1.6. The total polarization field (first and second order) that oscillates at frequency ω is

$$P_\omega = \chi^{(1)} E_\omega + \chi^{(2)} \left[2E_o E_\omega \right] \tag{1.2.4}$$

where propagation terms have been omitted for ease of calculation. This polarization produces a displacement field

$$\begin{aligned} D_\omega &= E_\omega + 4\pi P_\omega \\ &= E_\omega + 4\pi \left[\chi^{(1)} E_\omega + \chi^{(2)} \left(2E_o E_\omega \right) \right] \\ &= \left[1 + 4\pi\chi^{(1)} \right] E_\omega + 8\pi\chi^{(2)} E_o E_\omega \\ &= \left[1 + 4\pi\chi^{(1)} + 8\pi\chi^{(2)} E_o \right] E_\omega = \left[n_o^2 + 8\pi\chi^{(2)} E_o \right] E_\omega = \varepsilon E_\omega \end{aligned} \tag{1.2.5}$$

So the refractive index for this medium is

$$n_\omega = \sqrt{n_o^2 + 8\pi\chi^{(2)} E_o} \tag{1.2.6}$$

The refractive index at frequency ω is dependent on the applied DC field, and can be controlled by altering the magnitude of the DC field. This is known as the linear electro-optic effect (LEO) or as the Pockels effect.

One of the simplest applications of the electro-optic effect is in a Mach-Zehnder interferometer to modulate wave amplitude. An incident electric wave $E = E_o e^{i(kx - \omega t)}$ with intensity I_o is split into the two arms of the interferometer (Figure 1.2.1a) that is etched in an electro-optic medium (second order nonlinear optical medium), with equal lengths and refractive indices *n*. Since the arm lengths and refractive indices are equal, the optical path length down each arm is identical and the waves recombine constructively to

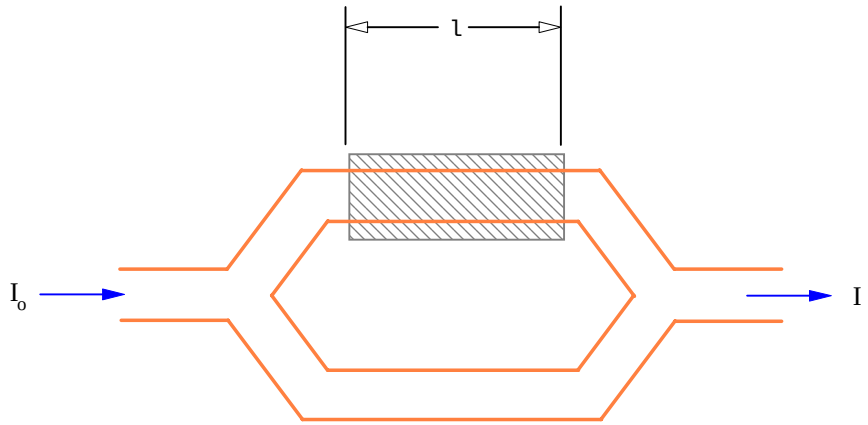

(a)

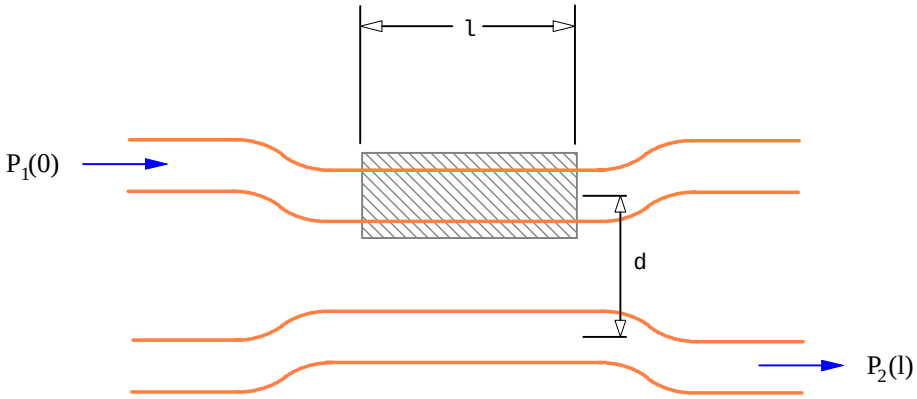

(b)

Figure 1.2.1: Applications of the linear electro-optic effect. (a) Mach Zehnder interferometer as a electro-optic switch and/or amplitude modulator (b) Directional coupler using evanescent coupling between adjacent waveguides with center-center distance *d*. In both cases electrodes of length *l* are positioned above and below the upper arm of the device.

obtain the initial intensity I_o. If the medium is a uniaxial crystal of the $C_{\infty v}$ structure, the ordinary refractive index n_o varies with a DC field E_{oz} applied in the direction of the extraordinary axis as

$$n_o'(E_{oz}) = n_o - \frac{1}{2} n_o^3 r_{33} E_{oz} \tag{1.2.7}$$

where r_{33} is the electro-optic coefficient associated with the medium. If the DC field is applied across electrodes of length l, a phase difference $\Delta\varphi$

$$\begin{aligned} \Delta\varphi &= \frac{2\pi l}{\lambda}(\Delta n) \\ &= \frac{\pi l}{\lambda} n_o^3 r_{33} E_{oz} \end{aligned} \tag{1.2.8}$$

is introduced, and the recombined wave becomes

$$E' = E_o \cos\left(\frac{\Delta\varphi}{2}\right) e^{i(kx-\omega t)} \tag{1.2.9}$$

with intensity

$$I = I_o \cos^2\left(\frac{\Delta\varphi}{2}\right) \tag{1.2.10}$$

Given electrode spacing d (above and below the waveguide arm) and potential difference V, the voltage for a phase shift of π is

$$V_\pi = \frac{d\lambda}{l n_o^3 r_{33}} \tag{1.2.11}$$

The interferometer can act as an on/off switch for $V=0$ (maximum intensity) and $V=V_\pi$ (zero intensity), or as an amplitude modulator for intermediate voltages.

The above-mentioned electro-optic coefficient, r, is a third-rank tensor that relates the displacement field $\vec{D}$ in a medium to the electric field $\vec{E}$ (the inverse relationship that corresponds to eq. 1.2.2). For lossless media, the permittivity tensor ε_{ij} is real and symmetric and its inverse must also be real and symmetric. This causes r_{ijk} to be symmetric in its first two indices. We can then contract the electro-optic tensor r_{ijk} to a two dimensional matrix r_{hk}, where the contracted subscript h corresponds to the following subscripts ij: h=1 for ij=11, h=2 for ij=22, h=3 for ij=33, h=4 for ij=23 or 32, h=5 for ij=13 or 31, h=6 for ij=12 or 21.

We can then relate the change in refractive index to the electro-optic coefficients[3] and the applied electric field as

$$\Delta\left(\frac{1}{n^2}\right)_i = \sum_j r_{ij} E_j \tag{1.2.12}$$

We can rewrite this change in refractive index as

$$\Delta\left(\frac{1}{n^2}\right) = \frac{d}{dn}\left(\frac{1}{n^2}\right) = \frac{-2}{n^3}\frac{d}{dn}(n^2) = \Delta n^2 \tag{1.2.13}$$

We can rewrite eq. 1.2.6 as

$$\begin{aligned} n_\omega^2 - n_o^2 &= 8\pi\chi^{(2)} E_o \\ \Delta n^2 &\propto \chi^{(2)} E_o \end{aligned} \tag{1.2.14}$$

Inspection of eqs. 1.2.12, 1.2.13, and 1.2.14 indicate that the electro-optic coefficient is then linearly related to the second-order nonlinear susceptibility $\chi^{(2)}$.

As a second application, consider two parallel waveguides with electric fields polarized in y and propagating in z. The electric fields in the waveguides can be expressed as

$$\begin{aligned} E_1 &= \tilde{E}_1 u_1(y) e^{-i\beta_1 z} \\ E_2 &= \tilde{E}_2 u_2(y) e^{-i\beta_2 z} \end{aligned} \tag{1.2.15}$$

Where $u_i(y)$ are transverse spatial modes of the waves and β_i are propagation constants dependent on wavelength and refractive index. When the separation distance d between two such waveguides is sufficiently small, the fields may weakly couple due to evanescent waves at the waveguide boundaries (Figure 1.2.1b). This implies that wave amplitudes may vary but that spatial modes will remain constant[4]. If the intensity at z=0 is $I_1(z=0) = I_o$ and $I_2(z=0) = 0$, it can be shown that the intensity at arbitrary z is

$$\begin{aligned} I_1(z) &= I_o\left[\cos^2 \gamma z + \left(\frac{\Delta\beta}{2\gamma}\right)^2 \sin^2 \gamma z\right] \\ I_2(z) &= I_o \frac{|C|}{\gamma^2} \sin^2 \gamma z \end{aligned} \tag{1.2.16}$$

where C is a coupling coefficient which is a function of waveguide dimensions, refractive indices, wavelength, and spatial modes, and

$$\gamma^2 = \left(\frac{\Delta\beta}{2}\right)^2 + C^2$$
$$\Delta\beta = \beta_1 - \beta_2 = \frac{2\pi\Delta n}{\lambda} \tag{1.2.17}$$

If the refractive indices are equal, $\Delta\beta=0$ and the intensities can be written

$$I_1(z) = I_o \cos^2 cz$$
$$I_2(z) = I_o \sin^2 cz \tag{1.2.18}$$

and total power will transfer from waveguide 1 to waveguide 2 over a distance

$$L_o = \frac{\pi}{2C} \tag{1.2.19}$$

The device is fabricated such that the total power transfer when no voltage is applied is

$$T = \left(\frac{\pi}{2}\right)^2 \operatorname{sinc}^2\left\{\frac{1}{2}\left[1+\left(\frac{L_o\Delta\beta}{\pi}\right)^2\right]^{\frac{1}{2}}\right\} \tag{1.2.20}$$

which has zeros at $L_o\Delta\beta = \pm\sqrt{3}\pi$. With particular choices of waveguide dimension and spacing, a voltage necessary to prevent power transfer by spoiling the refractive index can be calculated. This allows an electro-optic 'switch' to be constructed that transfers total energy from one waveguide to another with zero applied voltage and retains energy in the original waveguide by the application of a DC field.

Because of applications such as those described here, there is a great interest in the development of improved $\chi^{(2)}$ materials.

1.3 Second Order Nonlinear Materials

Of foremost concern in second order nonlinear optical materials is a requirement for non-centrosymmetry in the material structure. This can be illustrated by considering an electric field

$$E(t) = E_{\omega} \cos \omega t \tag{1.3.1}$$

incident on a centrosymmetric medium. The resultant second order polarization for this medium is

$$P(t) = \chi^{(2)} E^2(t) \tag{1.3.2}$$

It the medium is centrosymmetric it must possess inversion symmetry, where

$$\begin{aligned} -P(t) &= \chi^{(2)} \left[-E(t)\right]^2 \\ -P(t) &= \chi^{(2)} E^2(t) \end{aligned} \tag{1.3.3}$$

Equations 1.3.2 and 1.3.3 hold simultaneously only when the polarization field is zero, indicating $\chi^{(2)}=0$ for centrosymmetric media. This requirement can be further illustrated by considering the induced dipole moment of a molecule in a sinusoidal electric field (Figure 1.3.1a). Both linear media and nonlinear, centrosymmetric media yield polarization fields that are symmetric in space and therefore exhibit a zero time-averaged response. Only a non-centrosymmetric nonlinear medium can exhibit a nonzero time-averaged polarization field (Figure 1.3.1d).

Such non-centrosymmetric media have generally been obtained through the use of inorganic crystals. Potassium dihydrogen phosphate (KDP), β-barium borate (BBO) and lithium niobate (LNB) are examples of these, and are frequently incorporated into high-power applications. These crystals exhibit $\chi^{(2)}$ values on the order of $1\text{-}100 \times 10^{-9}$ esu, arising from the electron polarizability due to the crystal's band structure and the asymmetry associated with the crystal structure. Crystal growth procedures are complicated and time consuming, requiring precise variational control of temperatures between 600 and 1000 degrees Celsius at extreme pressures (high vacuum or inert atmosphere at up to 1700 atm)[5]. Growth times can range from 10 days to 8 weeks, and produce crystals of dimension 20mm x 20mm x 60mm. Material design is difficult, reducing the ability to tailor new crystals to specific needs. Many inorganic crystals show moderate to poor environmental stability, exhibiting particular weakness to atmospheric humidity.

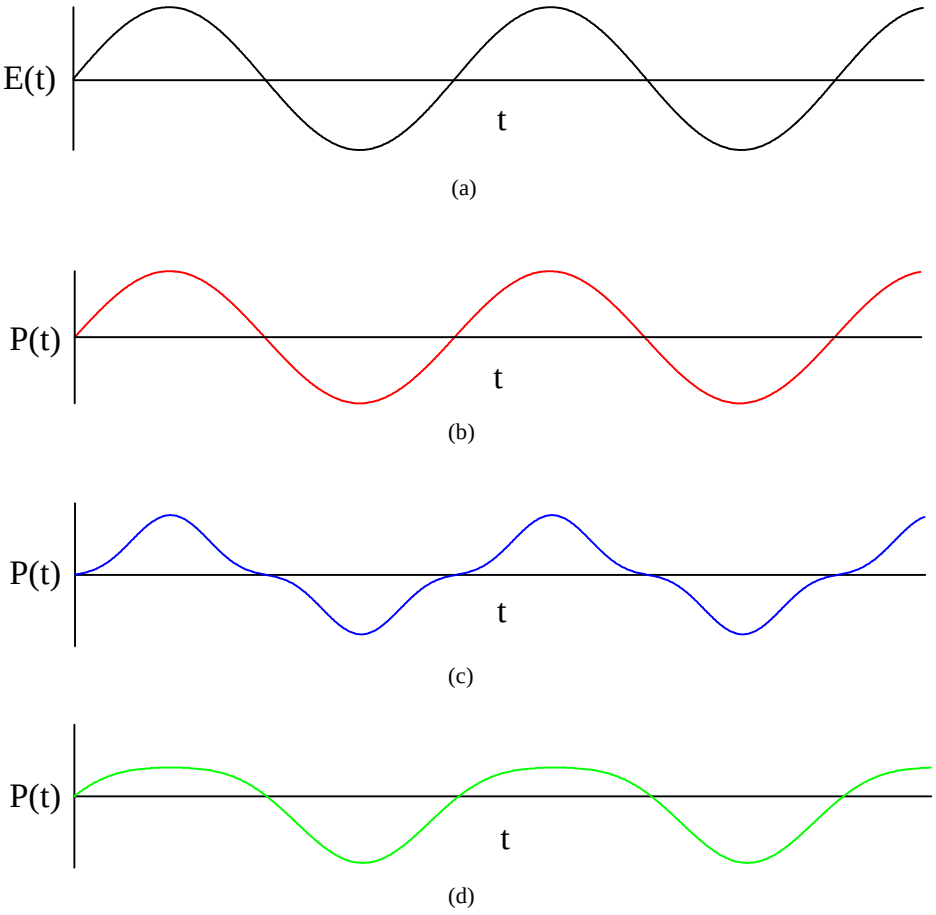

Figure 1.3.1: Electric field and corresponding polarization fields in various media. (a) Incident electric field. (b) Polarization field of (a) in linear, centrosymmetric medium. (c) Polarization field of (a) in centrosymmetric, nonlinear medium. (d) Polarization field of (a) in noncentrosymmetric, nonlinear medium. Only (d) has non-zero time-averaged polarization field (and non-zero $\chi^{(2)}$)

Organic Chromophores

As an alternative to inorganic crystals, organic molecules and polymers have been of considerable interest for use in nonlinear optics due to their large optical nonlinearities. The dipole moment of such a molecule can be expanded as a Taylor series in the same manner as the polarization field in eq. 1.1.4b. This results in a dipole moment with higher-order corrections

$$\begin{aligned} p_i(\omega) = \mu_i + \alpha_{ij}(-\omega)E_j(\omega) + \beta_{ijk}(-\omega;\omega_1,\omega_2)E_j(\omega_1)E_k(\omega_2) \\ + \gamma_{ijkl}(-\omega;\omega_1,\omega_2,\omega_3)E_j(\omega_1)E_k(\omega_2)E_l(\omega_3) + \ldots \end{aligned} \tag{1.3.4}$$

where β_{ijk} and γ_{ijkl} are the first- and second-order molecular hyperpolarizabilities associated with the second and third order nonlinear optical effects, respectively. For a collection of N molecules, the second order nonlinear susceptibility $\chi^{(2)}$ can be expressed as an orientational average over the molecules and their hyperpolarizability β_{ijk}

$$\chi^{(2)}_{ijk}(-\omega;\omega_1,\omega_2) = N\sum\left\langle R_{i\mu}R_{j\nu}R_{k\rho}\right\rangle\beta_{\mu\nu\rho}\, f(\omega)\, f(\omega_1)\, f(\omega_2) \tag{1.3.5}$$

where *R*'s are direction cosines between lab axes (*i*,*j*,*k*) and molecular axes (μ,ν,ρ) and *f*'s are local field factors representing corrections to the electric field experience by each molecule due to the electric fields of its neighbors.

Large molecular hyperpolarizabilities require highly polarizable electrons (to be able to respond to an electric field) and asymmetry on the molecular level. Large polarizability is achieved through conjugation, where π electron bonds between unsaturated atoms in organic compounds are delocalized and easily moved by electric fields. Asymmetry is provided through the use of electron donor and acceptor groups attached at opposite ends of the molecule[6]. These groups provide a permanent dipole moment, which causes the resulting induced moment to be asymmetric. Analogous to the first order dipole moment of two static charges, increasing the strength of the donor /acceptor groups and increased conjugation length between these groups generally results in larger hyperpolarizabilities as illustrated in Table 1.3.1[7].

Table 1.3.1: Hyperpolarizabilities β_0 and structures of selected organic chromophores. β_o indicates primary component of hyperpolarizability, with all field polarizations aligned with long axis of molecule.

Chromophore	Structure	β_o (10^{-30}cm^5/esu)
DMNA	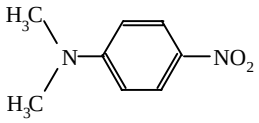	12
NB-DMAA	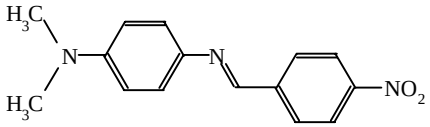	37
Disperse Red 1	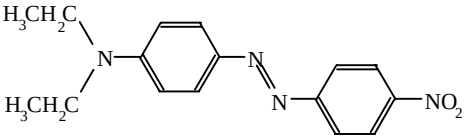	47
DMA-NS	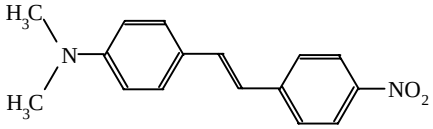	52
DMA-DCVS	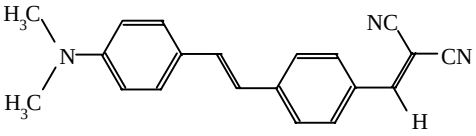	133
DEA-TCVAB	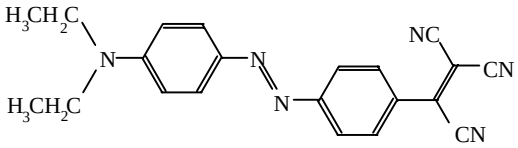	154

The first-order hyperpolarizability β can be measured by several techniques. Most common is the electric-field induced SHG (EFISH) method[8]. An electric field is used to align the chromophores in solution, producing an asymmetric medium for a second harmonic generation measurement. A comparison with a reference sample, generally quartz, allows a calculation of β. When the chromophore in question possesses ionic groups, the EFISH method results in a separation of chromophore from solution (literally 'plating' the field electrodes). In these cases, the method of Hyper Rayleigh scattering (HRS)[8] is used. HRS measures incoherently scattered SHG from even isotropic solutions. Coherent SHG intensity is proportional to the square of $\langle\cos^3\theta\rangle$, with molecular orientation angle θ. If the sample is completely isotropic, this result is zero. Scattered SHG intensity, however, depends only on $\langle\cos^2\theta\rangle^2$, which is nonzero even for random orientation. Analysis of the polarization of scattered second harmonic with respect to the polarization of the incident fundamental allows resolution of β_{zzz} and β_{zxx} components of the hyperpolarizability.

Guest-Host Polymers

The most general method of utilizing these molecules for $\chi^{(2)}$ applications is through polymer films fabricated by mechanical techniques such as spin-casting. Chromophores are doped into an optically inactive polymer and deposited on a substrate. The deposition leaves the chromophores with randomized orientation and therefore with zero $\chi^{(2)}$. In order to make useful $\chi^{(2)}$ materials, these films are heated above their glass-transition temperatures (in many cases ~100°C-200°C), allowing the chromophores some degree of orientational mobility. A strong electric field is applied (typ. $\sim 10^5$-10^6 V/m) to 'pole' the chromophores, aligning them with the electric field. The field is maintained as the film is cooled down below its transition temperature, effectively 'freezing in' the chromophore alignment. This process, producing what are known as 'poled polymers', yields typical $\chi^{(2)}$ values of 10^{-8} to 10^{-7} esu[9]. For comparison, BBO, one of the commonly used $\chi^{(2)}$ crystal materials, has a value of $9.2*10^{-9}$ esu. Unfortunately, the chromophore orientation of poled polymers tends to decay over time due to randomization of chromophore alignment. For example, at room temperature, the second order susceptibility in some guest-host systems has shown a sharp initial decay (10-50% in the first 24 hours) followed by a slower decay (20% over a year)[10]. This

decay rate is increased as temperatures approach the glass transition temperature, at which point decay is nearly instantaneous. This decay has been diminished by covalent attachment of the chromophore to the polymer and through the use of cross-linking polymers. When exposed to UV radiation, bonds are formed between photo-reactive groups present on the polymers, reducing the orientational mobility of the polymer. When poled, crosslinked polymers can show smaller $\chi^{(2)}$ than uncrosslinked polymers (1.1×10^{-7} esu vs. 1.6×10^{-7}esu, respectively, for example[11]) but show reduced decay rates (10% vs. 50% over 500 hours at room temperature) due to this reduction of orientational mobility.

Further increases in orientational stability have been achieved through the use of polyimides to reduce orientational mobility in poled polymers[12,13]. As shown in Figure 1.3.2a, chromophores are doped into polyamic acid (they may also be covalently attached as side-groups) and deposited (spin coated) onto a substrate. A poling field is applied, orienting the guest chromophores. Simultaneously, the film is heated to above T_g (>250°C), which causes the polyamic acid to condense to form imide rings (Fig. 1.3.2c). This imidization restricts the allowed motion of the chromophores and increases the thermal stability of the films. Because the formation of each imide ring produces a water molecule, a final curing step (called densification) is taken at higher temperature (~350°C) to decrease the moisture content of the films. This can result in a decrease in film thickness by 40%[12], further limiting the reorientational mobility of the guest chromophores. This densification has been shown to be crucial to the increased thermal stability exhibited by these films[13]. It is only after cooling to room temperature after this final curing step that the poling field is removed. This process has resulted in films that exhibit relatively good thermal stability at high temperatures. It is important to note, however, that the necessary processing temperatures are generally above thermal breakdown temperatures of most nonlinear chromophores.

Langmuir-Blodgett Deposition

In order to avoid the orientational relaxation (depoling) that occurs in poled polymers, various attempts have been made to fabricate nonlinear films with an intrinsic structural asymmetry. These self-assembly

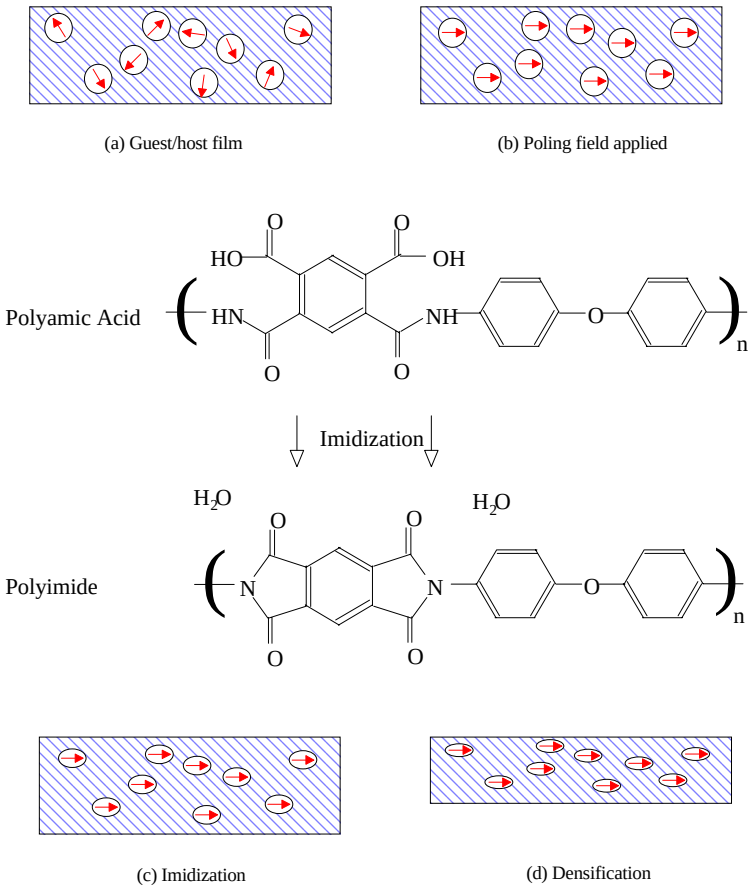

Figure 1.3.2: Post-processing of polyimide films. (a) Guest/host polyamic acid film. Poling field is applied in (b), orienting chromophores. Imidization occurs in (c), restricting chromophore mobility. Excess moisture from imidization is driven out in densification (d), further restricting chromophore mobility

techniques involve molecules that are aligned by the deposition procedure itself. They generally fall into two categories – Langmuir-Blodgett deposition and covalent self-assembly.

In the simplest form of Langmuir-Blodgett deposition, molecules that are hydrophilic on one end and hydrophobic at the opposite end are spread on a water surface. This layer is then compressed until the molecules are close packed (and therefore aligned). This is the formation of the actual monolayer. In order to transfer this monolayer onto a substrate, a substrate is immersed in the water through the monolayer in a vertical orientation (Figure 1.3.3a). If the substrate is hydrophobic, the first layer will be formed upon immersion. When the substrate is removed, a second layer is deposited on top of the first. When a monolayer is transferred to the substrate on both immersion and removal, the resulting structure is called 'Y-Type'. Most L-B capable molecules form this type structure. X- and Z-Type structures are formed when monolayers are deposited on insertion or withdrawal only. Both X- and Z-Type structures possess an inherent structural asymmetry, as molecules in adjacent layers are oriented head-to-tail. Z-Type films have been shown to produce nonlinear susceptibilities approximately 10 times that of β-barium borate[14]. Though Y-Type structures are inherently structurally symmetric, several tricks may be played to obtain films with non-zero $\chi^{(2)}$. For example, molecules can be chosen which exhibit non-zero hyperpolarizability in the plane of the monolayer[15,16]. In a slightly more complicated arrangement, a net orientation perpendicular to the substrate is possible by utilizing two different L-B films. The substrate is immersed through a non-absorbing, nonlinear inactive molecular monolayer, adsorbing the first layer. The substrate is then moved while immersed through a gate and into a second water bath, where it is withdrawn through a monolayer that contains an NLO chromophore. Though a Y-Type structure is formed, the chromophores exist only on the withdrawal monolayer, behaving as a Z-Type structure. Films deposited in this fashion have shown non-linear susceptibilities of $\chi^{(2)}=16*10^{-7}$, roughly 20 times larger than that of β-barium borate[17].

Langmuir-Blodgett deposition is complicated by the need to maintain a constant surface pressure of the molecules during insertion and removal. Since that pressure causes the molecules to be close-packed, if pressure is decreased molecules are allowed to relax their orientation. If pressure is too high, the

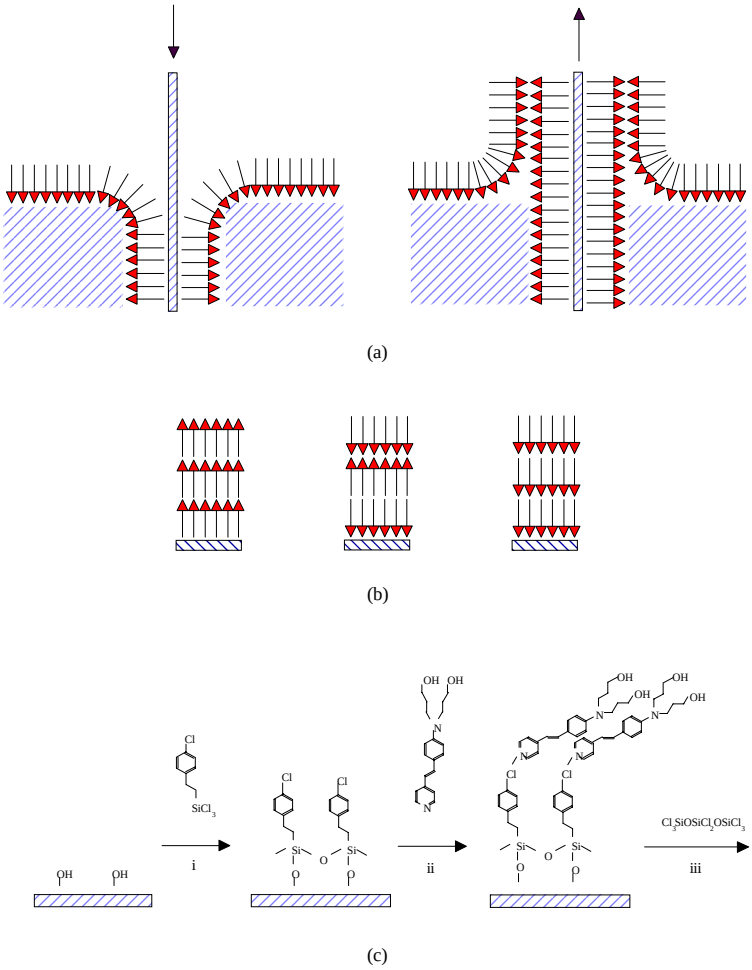

Figure 1.3.3: Langmuir-Blodgett and covalent self-assembly processes. (a) Deposition of Langmuir-Blodgett molecules (hydrophilic ends represented as arrowheads) on a hydrophobic substrate. Deposition occurs both on substrate insertion and removal (Y-Type). (b) X, Y, and Z type L-B films. (c) Covalent self-assembly process of (dialkylamino) stilbazole onto benzyl chloride surface. Step (iii) crosslinks hydroxy groups and serves as activation for deposition of next layer, beginning at step (i)

monolayer can break down with molecules folding on top of each other. Constant pressure is generally maintained by a series of compression and removal rollers in the bath in conjunction with the application of 'piston oils', which serve to apply pressure to the L-B molecules[18]. The deposition apparatus and procedure is complicated and sensitive to environmental conditions and contaminants.

Perhaps most significantly, Langmuir-Blodgett films show poor mechanical and thermal stability due to the van Der Waals interactions between layers. The few X- and Z-Type molecules commonly decay to Y-Type structures, destroying the asymmetry[18]. Increased heat and elapsed time serves to collapse Langmuir-Blodgett layers, randomizing any chromophore orientation. It is worth noting that L-B films incorporating polyimides to stabilize structure have been investigated and appear to possess some amount of thermal stability up to 240°C[16], but $\chi^{(2)}$ measurements have not been made on these films.

Covalent Self-Assembly

Covalently self-assembled films, commonly known as self-assembled monolayers (SAMs) or chemisorbed films, overcome several of the drawbacks of Langmuir-Blodgett films. In this method, hydroxylated substrates are immersed in an amphophillic fluid (solution, melt, or vapor) and a thermodynamically stable film is covalently bonded to the surface. This layer may be followed by alternating steps which chemically activate the new surface layer and then deposit further layers[19] (Figure 1.3.3c). In this process, highly organized multilayer structures may be fabricated. SAM films show exceptional mechanical, chemical, and electrical stability, and may be cross-linked to further increase these characteristics[20]. The organization of these structures is particularly conducive to producing $\chi^{(2)}$ materials, and films have been produced with second order susceptibilities of up to $6.0*10^{-7}$esu[21], over 60 times that of β barium borate, a crystal commonly used for second harmonic generation and optical parametric oscillation applications today.

Production of covalently self-assembled films is extremely time consuming. Immersion times per layer may range from 4 hours to several days[22]. Both adsorption and layer activation steps must, in general, be

conducted at elevated temperatures[23]. These factors are aggravated by the necessity of 100% reactance of the surface layer in order to assure proper molecular orientation.

Ionic Self-Assembled Monolayer (ISAM) Technique

A new deposition technique that has been shown to bypass many of the problems of these other methods was first demonstrated by G. Decher and coworkers in 1991[2]. The technique, referred to here as ionic self-assembled monolayers (ISAM), utilizes the coulombic attraction between oppositely charged polymers to form ultrathin layers of organic polymers in a precisely controlled fashion. The deposition process involves the immersion of a charged substrate into an oppositely charged aqueous polyelectrolyte solution. As the polyelectrolyte forms ionic bonds with the substrate surface, some fraction of the ionic groups extends away from the substrate. These groups cause an effective reversal of the surface charge, which limits further polyelectrolyte adsorption. The substrate is removed from solution at this point, rinsed with pure water to remove unbonded polymer, and immersed in a second aqueous polyelectrolyte solution of opposite charge to the first. The process repeats, with polyelectrolyte adsorption again reversing the surface charge. This process can be repeated in the $(AB)_n$ fashion until desired film thickness is obtained. Since deposition requires only that successive layers have opposite ion charge (anion/cation), it is possible to construct films whose structure is more complicated than the $(AB)_n$ bilayer repeat unit. Films with $(ABAC)_n$ structures[24], for example, have been fabricated and other structures are also possible. This allows polymer layers with different functionality to be easily incorporated into a single film with precise structural control

The subject of this thesis is the exploration of ISAM deposition to provide inherently noncentrosymmetric $\chi^{(2)}$ films. In addition to absorbance and film thickness measurements, we will use second harmonic generation to give us information on chromophore orientation within the film. We will present results which show that ISAM films are easier to design and fabricate than other self-assembled films, and exhibit better thermal characteristics than guest-host polymer films.

Chapter Two describes the ISAM deposition process in detail. We discuss the particulars of the thin film fabrication technique and some of the general characteristics of ISAM films produced for this study. We discuss some basic tenets of polymer adsorption from solution in order to arrive at some particulars of polyelectrolyte adsorption. Various deposition parameters such as solution acidity and ionic strength and their role in film formation are also investigated. The last section in Chapter Two discusses a brief investigation into the kinematics of ISAM deposition.

Chapter Three presents the characterization of the second order non-linear optical responses of ISAM films. The second harmonic generation (SHG) apparatus is discussed, including a brief description of the optical parametric oscillator used in the experiments. A comparison of SHG in ISAM films to that observed in Maker fringes in quartz provides an absolute standard for $\chi^{(2)}$ values. Second harmonic generation is then used as a tool for film characterization, both to determine the consistency of the structure over increased numbers of adsorbed bilayers and to determine chromophore orientation within the film. This chapter ends with a series of studies of SHG in ISAM films at elevated temperatures. As significant thermally-induced relaxation of $\chi^{(2)}$ is observed in other film deposition processes, the stability and recovery of ISAM films at high temperatures is of utmost interest.

Chapter Four discusses three possible approaches for improving asymmetry in ISAM films, thus improving second-order susceptibility. First we investigate the use of tailor-made polymers that have been designed to possess large hyperpolarizabilities and incorporate well into the ISAM structure. Secondly we will look at improving chromophore orientation through the use of cyclodextrin complexes, 'sleeves' which fit around chromophores, screening them from neighboring charges and potentially reducing the chromophore tilt angle. Thirdly, we investigate the use of dianionic chromophores in an ISAM film in order to reduce order competition between layer interfaces.

Finally, in Chapter Five, summaries of the investigation are given, and some possibilities for further study are offered.

[1] P. A. Franken, A. E. Hill, C. W. Peters, G. Weinreich, *Phys. Rev. Lett.*, **7**, (1961), p118-119

[2] G. Decher, J.D. Hong, *Thin Solid Films*, **210/211**, (1992) p831-835

[3] R. W. Boyd, Nonlinear Optics, Academic Press, Rochester, New York (1992)

[4] B. E. A. Saleh, M. C. Teich, Fundamentals of Photonics, Wiley, New York (1991) p 264

[5] J. D. Bierlein, H. Vanherzeele, *J. Opt. Soc. Am. B*, **6**, (1989), p622-633

[6] A. Garito, R. Shi, M. Wu, *Physics Today*, May, (1994), p51-57

[7] K. D. Singer in Polymers for Lightwave and Integrated Optics, L. A. Hornak, ed., Marcel Dekker, Inc., New York (1992), p321-342

[8] H. S. Nalwa, S. Miyata, Nonlinear Optics of Organic Molecules and Polymers, CRC Press, Boca Raton, (1997

[9] L. Cheng, R. Foss, G. Meredith, W. Tam, F. Zumsteg, *Mat. Res. Soc. Symp. Proc*., **247**, (1992), p27-39

[10] P. Pantellis, J. Hill in Polymers for Lightwave and Integrated Optics, L. A. Hornak, ed., Marcel Dekker, Inc., New York (1992), p343-363

[11] R. Jeng, Y. Chen, B. Mandal, J. Kumar, S. Tripathy, *Mat. Res. Soc. Symp. Proc*., **247**, (1992), p111-117

[12] J. Wu, J. Valley, S. Ermer, E. Binkley, J. Kenney, G. Lipscomb, R. Lytel, *Appl. Phys. Lett.*, **58**, (1991), p225-227

[13] J. Wu, E. Binkley, J. Kenney, R. Lytel, A. Garito, *J. Appl.. Phys*., **69**, (1991) p7366-7368

[14] G. Ashwell, T. Handa, R. Ranjan, *J. Opt. Soc. Am. B*, **15**, (1998) p466-470

[15] H. Nakahara, W. Liang, H. Kimura, T. Wada, H. Sasabe, *J. Opt. Soc. Am. B.*, **15**, (1998) p458-465

[16] C. Jung, M. Jikei, M Kakimoto, *J. Opt. Soc. Am. B*, **15**, (1998) p471-476

[17] M. Eva, T. Tsutsui, S. Saito, New Developments in Construction and Functions of Organic Thin Films, Elsevier Science, New York, (1996)

[18] A. Ulman, Characterization of Organic Thin Films, Butterworth-Heinemann, Boston (1995)

[19] H. Lee, L. Kepley, H. Hong, S. Akhter, T. Mallouk, *J. Phys. Chem*., **92**, (1988) p2597-2601

[20] L. Netzer, J. Sagiv, *J. Am. Chem. Soc*., **105**, (1983) p674-676

[21] Z. Xu, T. Zhang, W. Lin, G. Wong, *J. Phys. Chem*, **97**, (1993) p6958-6960

[22] X. Yang, D. McBranch, B. Swanson, D. Li, *Mat. Res. Soc. Symp. Proc*., 392, (1995) p27-32

[23] D. Allan et. Al., *Mat. Res. Soc. Symp. Proc*., **247**, (1992) p779-786

[24] G. Decher, Y. Lvov, J. Schmitt, *Thin Solid Films*, **244**, (1994) p772-777